Outline

Nomenclature

The Myth of the Inverse-Compton Catastrophe

Compact Doubles and Recurrent Activity

Why "Compact Symmetric Objects"?

Problems with definition

A critical Case: PKS 1413+135

The need for a revised definition of CSOs

The Catalog

Nomenclature

In the '60s and early '70s there was only one way to get sub-arcsecond imaging of a reasonable sample of radio sources: IPS

Compact steep-spectrum and peaked-spectrum radio sources

Christopher P. O'Dea[1] · D. J. Saikia[2]

The low-frequency structure of powerful radio sources and limits to departures from equipartition

M. A. Scott and A. C. S. Readhead *Mullard Radio Astronomy*
Mon. Not. R. astr. Soc. (1977) **180**, 539–550 '3 0HE

New samples include thousands of PS and CSS sources (e.g., Callingham+ 2017)

The new samples cover a broader range of frequency (Callingham+ 2017, Hancock+2009) and extend down to lower radio power.

PS can have narrow spectra, so a range of wavelengths is required.
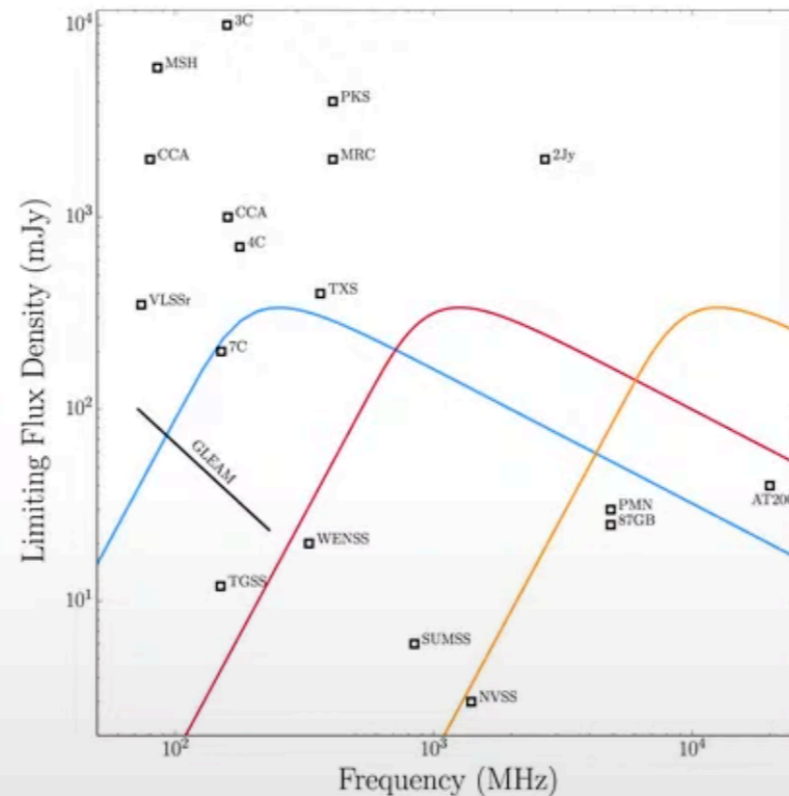
Comparison of parameter space of various radio surveys. (Callingham+2017).

Figure 3. The spectra of the three groups of sources: (a) sources having a spectral turnover near 81.5 MHz, (b) sources with flat or convex spectra over a wide frequency range, (c) steep spectrum sources with $\alpha \sim$ constant around 81.5 MHz.

All CSS sources will turn over at some frequency, so we should extend O'Dea and Saikia definition of PS sources to include all CSS sources

Redshift range 0.005 - 3 - i.e. a factor 4 in frequency and 300 in comoving coordinate distance

The low-frequency structure of powerful radio sources and limits to departures from equipartition

M. A. Scott and A. C. S. Readhead *Mullard Radio Astronomy*
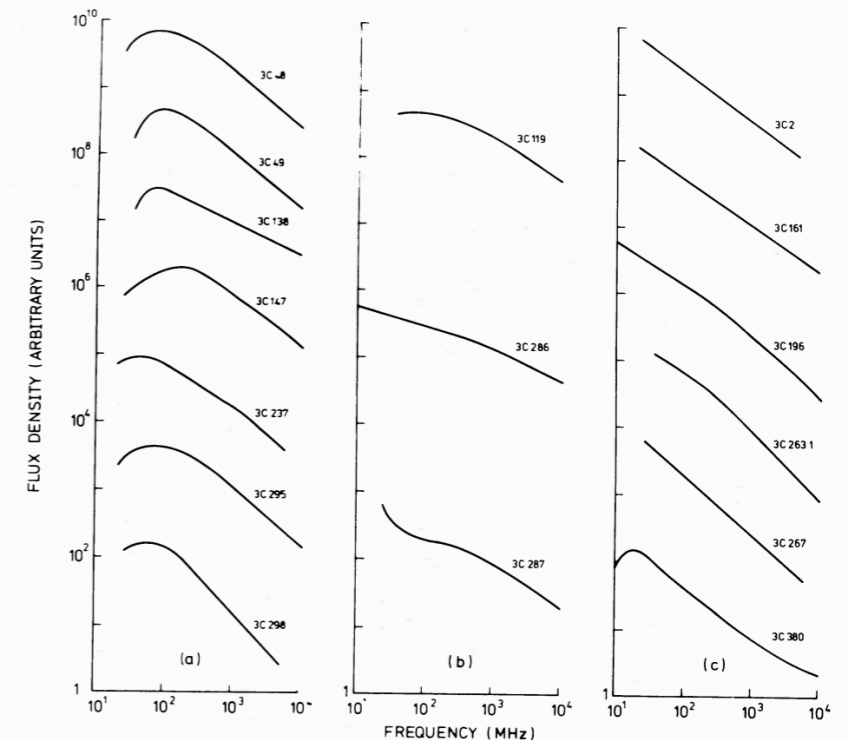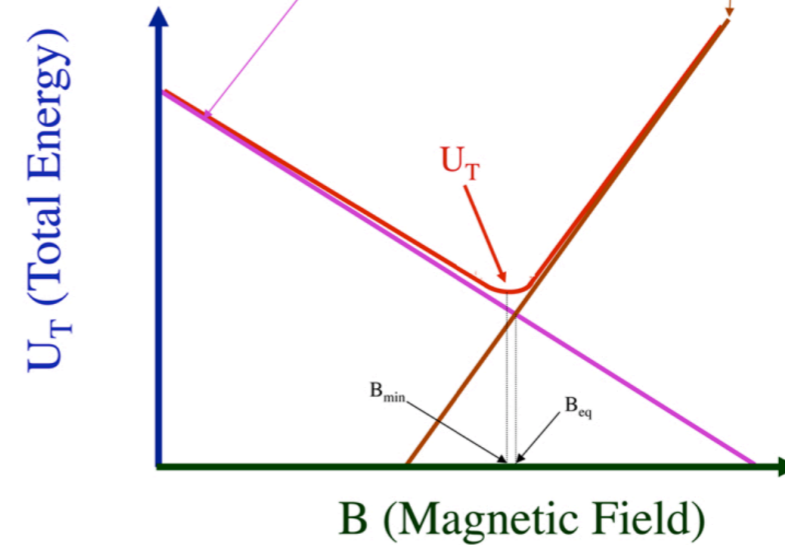*Mon. Not. R. astr. Soc.* (1977) 180, 539–550 '3 0HE

Figure 3. The spectra of the three groups of sources: (a) sources having a spectral turnover near 81.5 MHz, (b) sources with flat or convex spectra over a wide frequency range, (c) steep spectrum sources with $\alpha \sim$ constant around 81.5 MHz.

$$\psi_{eq} = 1.67 \times r^{-\frac{1}{17}} S^{\frac{8}{17}} \nu^{-\frac{35+2\alpha}{34}} (1+z)^{\frac{15-2\alpha}{34}} F(\alpha)$$

Magnetic field in powerful synchrotron sources

Burbidge & Burbidge 1957

1.

$$U_T = Ag(\alpha)LB^{-3/2} + VB^2/8\pi$$

U_T

B_{min} B_{eq}

B (Magnetic Field)

U_T (Total Energy)

2.
$$B_{SSA} \leq 1.0 \times 10^{-6} \left(\frac{S}{\psi^2}\right)^{-2} \nu^5 f_3(\alpha)^2 D ,$$

Table 1.

3C	ν_{peak} (MHz)	S_{peak} (Jy)	θ_{scint} (arcsec)	θ_{eq} (arcsec)	η	B_{eq} $(10^{-5}\,G)$	B_{est} $(10^{-5}\,G)$
							15
							3
							11
							2
							8

$$\theta \sim 5 \times \sqrt{S}/\nu, \text{ for } \nu \text{ in MHz, } S \text{ in Jy, and } \theta \text{ in arc seconds}$$

$$\nu \sim 5 \times \sqrt{S}/\theta \text{ for } \nu \text{ in MHz, } S \text{ in Jy, and } \theta \text{ in arc seconds}$$

★ Assuming an equal double at ν_{peak}.

FIG. 1a

FIG. 1b

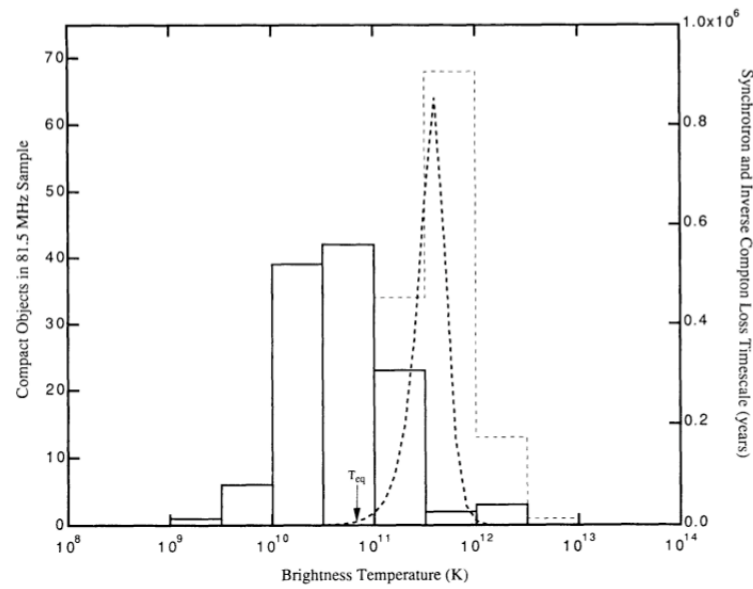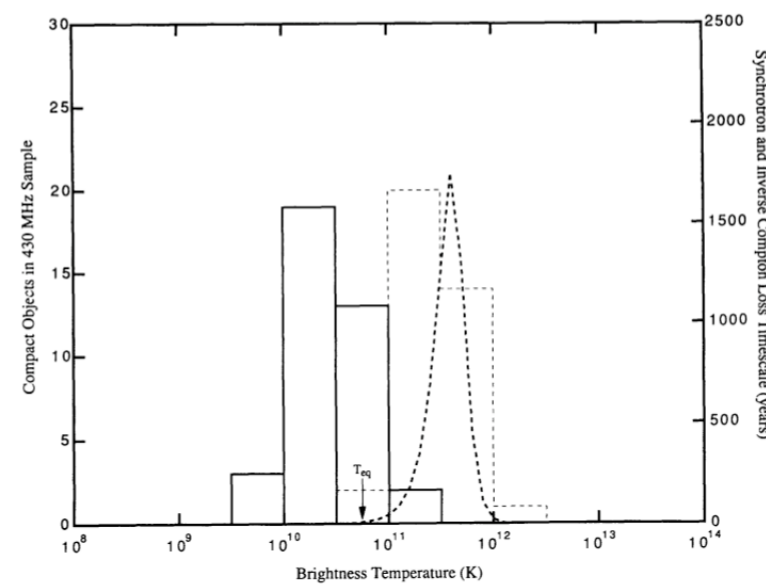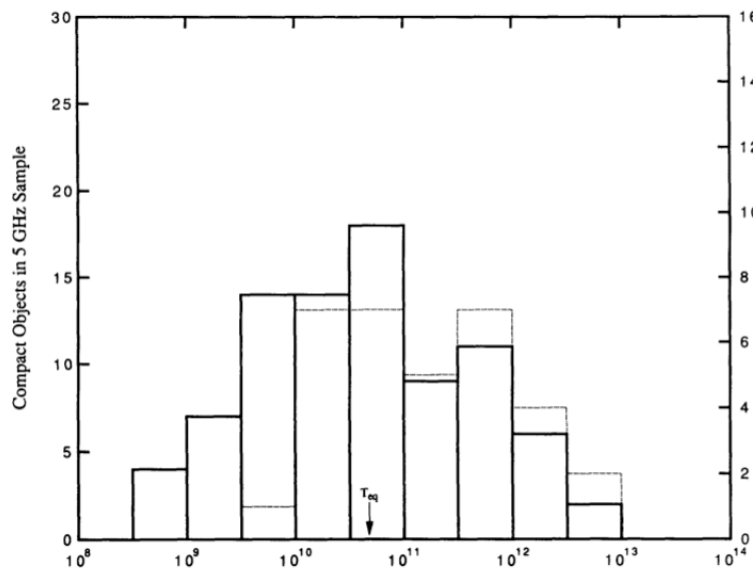majority of compact components detected in the survey have brightness temperature in the range 10^{10} K to 10^{11} K—well below the maximum observable brightness temperature.

The sensitivity of the interplanetary scintillation technique increases with decreasing angular size of the object, reaching a maximum for observations at 81.5 MHz at ~ 0.1 arc seconds—the limit imposed by interstellar scattering. Only objects smaller than $\sim 1''$ exhibit strong interplanetary scintillation at 81.5 MHz. Thus, in Figure 1a, the drop in numbers at small brightness temperature is due entirely to selection effects.

The upper cutoff in brightness temperature observed in this sample is clearly not due to selection effects, since the technique is more sensitive to more compact sources and we have corrected for interstellar scattering, so that there must be some other, physical, explanation for the cutoff at $T_b \sim 10^{11}$ K.

Broderick & Condon (1975) reached a similar conclusion when they studied the brightness temperatures in a complete sample of objects at 430 MHz.

The "Inverse ComptonCatastrophe is a Myth

The explanation for the inverse Compton catastrophe, which appears often to be misunderstood, is not so much that the photon energy density is increasing with T_b, since $u_{ph} \propto T_b$ (not a very strong dependence), but rather that the magnetic field energy density decreases dramatically with increasing T_b, as T_b^{-4}.

Compact Doubles

0108 + 388: a compact double source with surprising properties

S.A. Baum[1], C.P. O'Dea[1], D.W. Murphy[2,3], and A.G. de Bruyn[1]

[1] Netherlands Foundation for Research in Astronomy, Postbus 2, NL-7990 AA Dwingeloo, The Netherlands
[2] Nuffield Radio Astronomy Laboratories, Jodrell Bank, Macclesfield, Cheshire SK11 9DL, England
[3] Jet Propulsion Laboratory, 138-700, 4800 Oak Grove Drive, Pasadena, CA 91109, USA

Abstract. We present 49 cm and 6 cm WSRT and 20 cm VLA[1] observations of the candidate compact double radio galaxy 0108 + 388. In all three images we detect extended emission $\sim 20''$ (~ 60 kpc, assumed $z = 0.3$) to the east of the core. The emission is composed of a brighter peak of emission, surrounding diffuse emission, and a bridge of diffuse emission connecting to the core. This is the first detection of extended emission associated with a compact double galaxy.
It has been suggested that compact double sources are very young classical double radio galaxies ($\leq 10^4$ yr; e.g., Phillips and Mutel, 1982; Hodges and Mutel, 1987; Carvalho, 1985). The presence of radio emission tens of kpc from the nucleus of 0108 + 388 is inconsistent with a recent origin for the radio activity in this source. This apparent contradiction can be reconciled if the activity in this object is recurrent and the extended emission is the relic of a previous epoch of activity. Alternately, it may be that 0108 + 388 is not very young, but rather is a normal-aged radio galaxy in which most of the radio emitting plasma is currently unable to escape from the nuclear regions.
We also obtained 49 cm WRST observations of the 'proposed' compact double radio source, 2352 + 495. We detect no extended emission associated with 2352 + 495.
The spectrum of the core of 0108 + 388 exhibits a very steep turnover at low frequencies, with a spectral index of $\alpha > +2$. This property is probably related to the origin of the compact double.

sources reveal that some GPS sources (mainly quasars) exhibit complex morphologies. Others (mainly galaxies), termed 'compact double' (cd) sources, show two components of nearly equal flux density, similar spectral shapes and high brightness temperatures ($T_B \sim 10^{10}$ K) separated by tens of masec. Trails of diffuse emission are sometimes detected extending from the two components back towards the centroid of the double (Phillips and Mutel, 1980, 1982; Hodges, Mutel and Phillips, 1984; Mutel et al., 1985). The spectral turnover of the components of cds is naturally explained as the result of synchrotron self absorption in a single compact component with high magnetic fields and particle densities (e.g., Mutel et al., 1985).

The radio morphologies of cds, their high radio powers and extremely small extents, have led Phillips and Mutel (1980, 1982) to suggest that they represent the earliest stages in the development of powerful radio galaxies. Carvalho (1985) has produced models showing that the radio properties of cd sources are consistent with a scenario in which these sources represent the earliest stages ($t < 10^4$ yr) in the development of powerful classical double radio sources. In the proposed scenario, the cds then develop into compact steep spectrum radio sources with typical extents of 1–10 kpc and thereafter, on timescales of 10^7–10^8 yr into extended (10–1000 kpc) classical doubles.

We have begun a systematic study of the radio and optical properties of GPS radio sources. During the course of this investigation, we noticed that many of the GPS sources in the compilation of Gopal-Krishna et al. (1983) and Spoelstra et al.
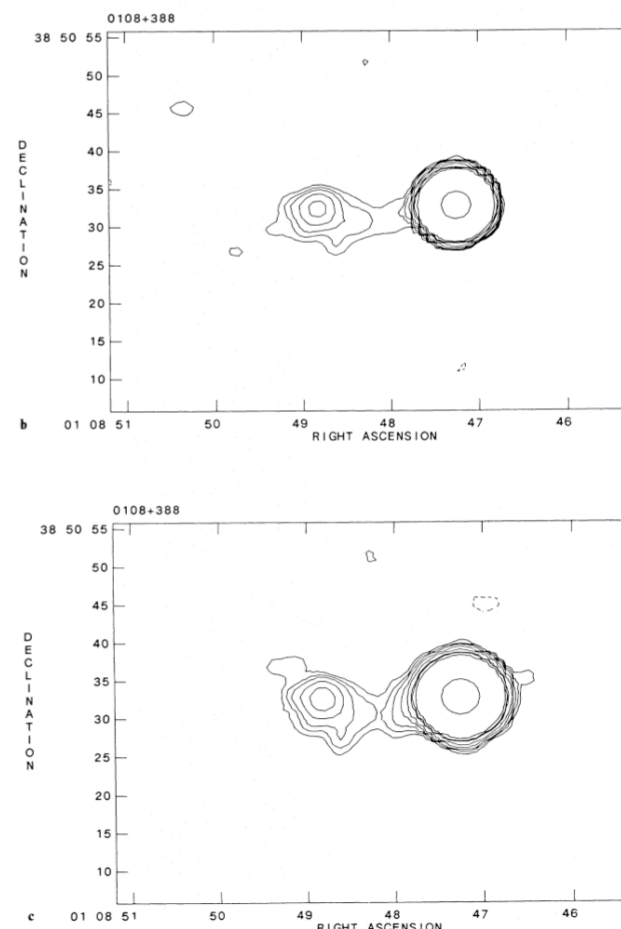

Fig. 3. a Contour plot of the 18 cm VLA A array image at full resolution (1.25 by 1.22, at position angle 73°, FWHM). Contours are at 2.5×10^{-4} Jy per beam, times (−3, 3, 5, 7, 10, 15, 25, 50, 250, 500, 1000); b Contour plot of the 18 cm VLA B array image at full resolution (4.15 × 3.8 at position angle 84° FWHM). Contours are at $3.0 \, 10^{-4}$ Jy per beam, times (−3, 3, 4, 5, 7, 10, 15, 20, 30, 1000); c Contour plot of the 18 cm VLA combined B and C array image at full resolution (4.55 by 4.2 at position angle 84°, FWHM). Contours are at $2.5 \, 10^{-4}$ Jy per beam, times (−3, 3, 4, 5, 7, 10, 15, 20, 30, 1000). The three images (a, b, c) are plotted with the same scale to facilitate comparison

Doesn't Recurrent, or Intermittent, Activity "Have" to be the explanation for the excess of compact, i.e. PS, sources?

Compact steep-spectrum and peaked-spectrum radio sources

Christopher P. O'Dea[1] · D. J. Saikia[2]
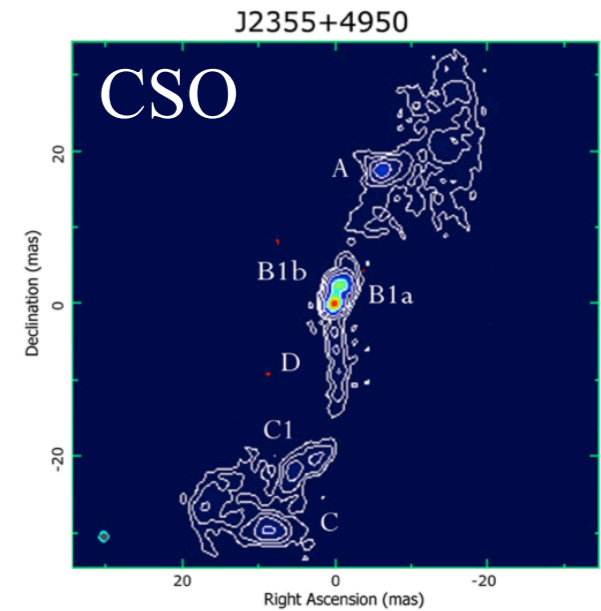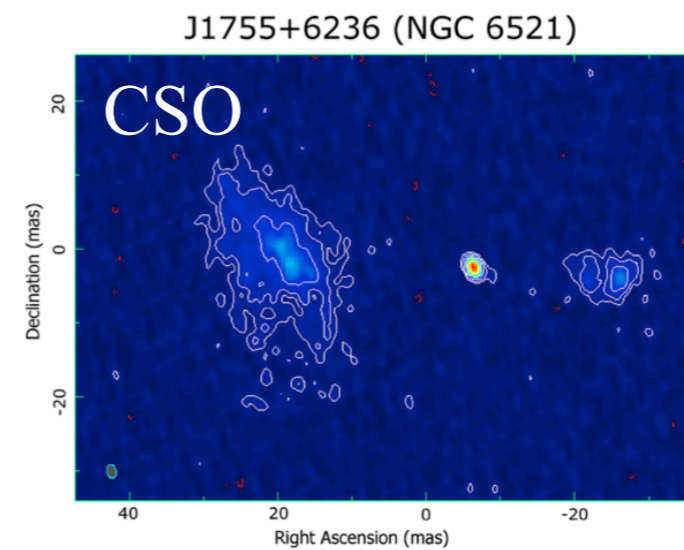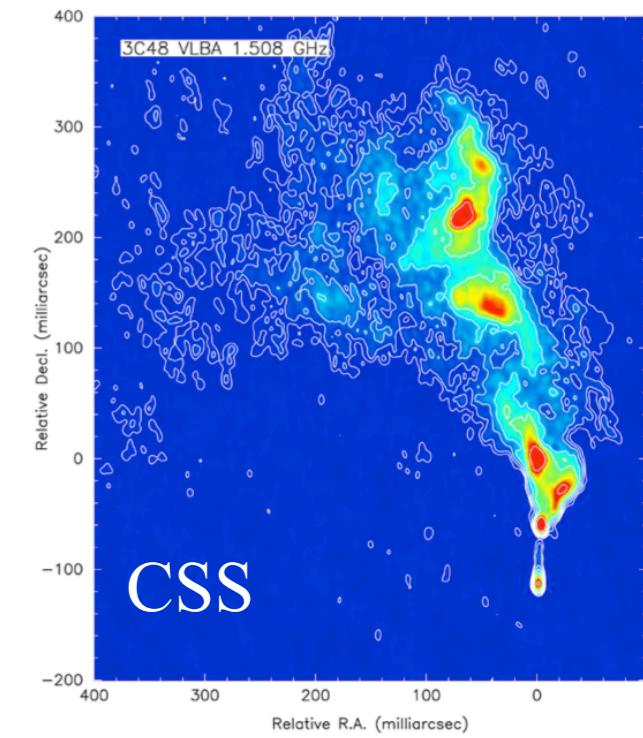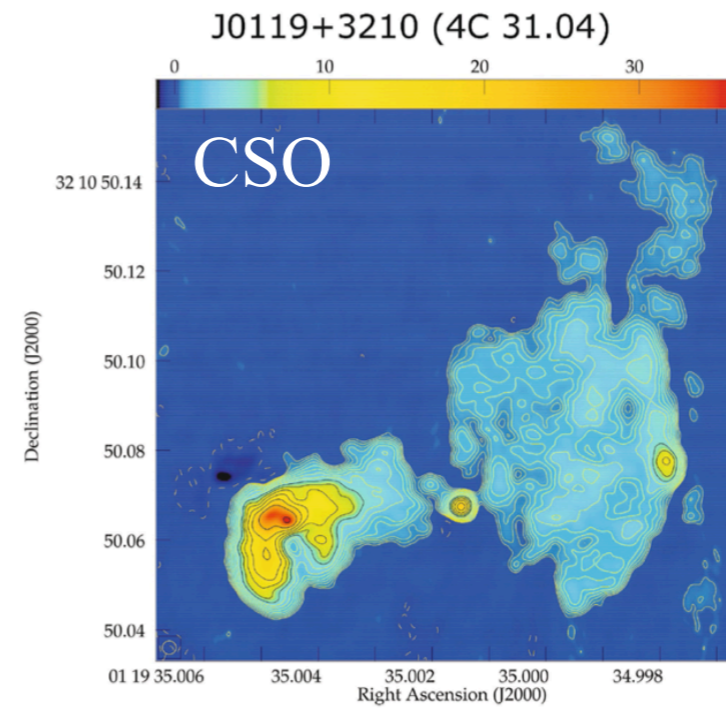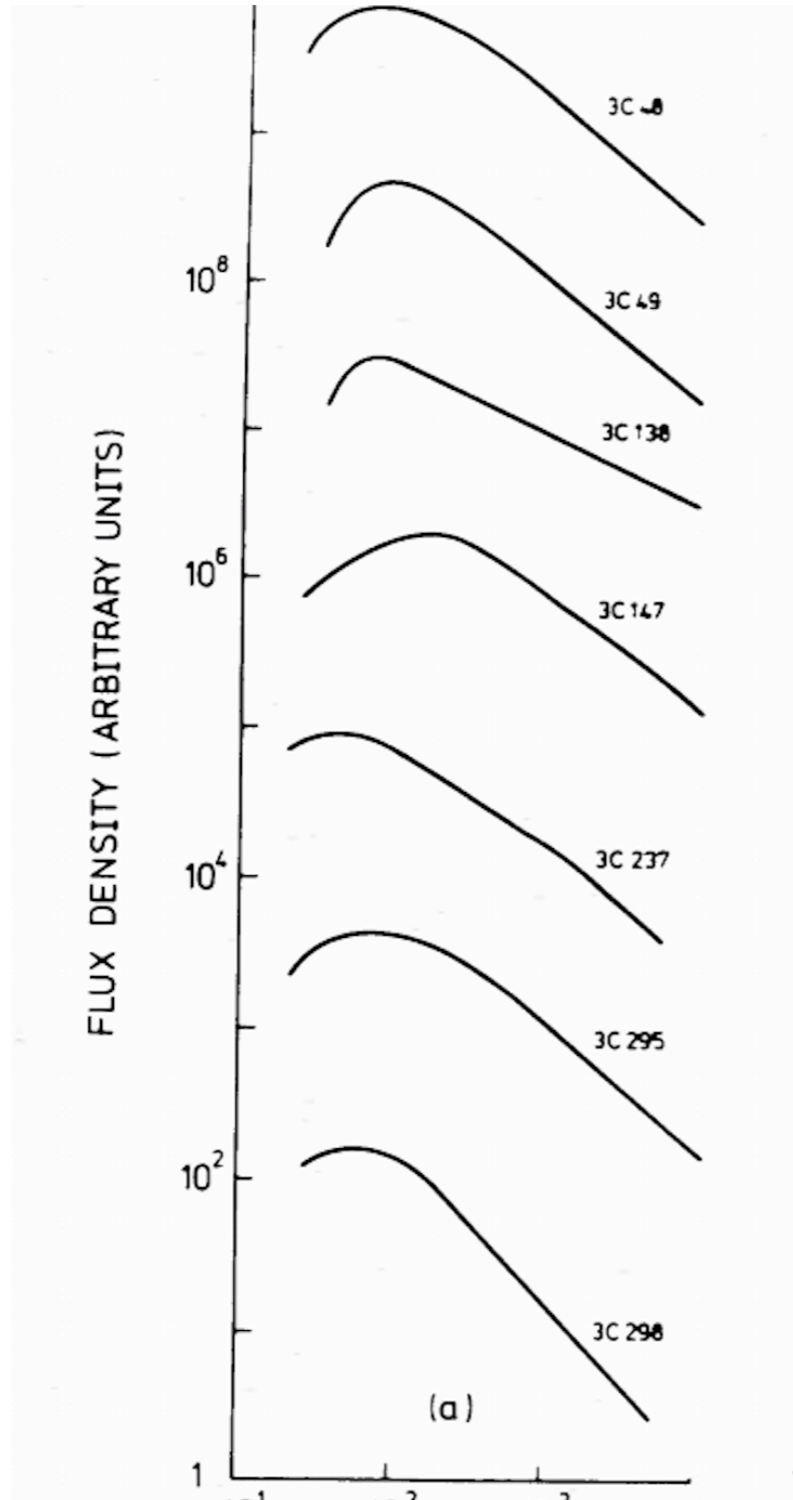
Fig. 1 Examples of structures of CSS/PS sources. Upper left: The CSO 4C31.04 (J0119+3210) which is associated with a galaxy at a redshift of 0.0602, has a peaked spectrum, and shows bright compact hotspots and extended emission on both sides along with a radio core (Giroletti et al. 2003). The projected linear size defined by the outer peaks of emission is 107 pc. Upper right: The CSS quasar 3C48 (J0137+3309) at a redshift of 0.367 which shows a disrupted jet indicating strong interaction with the interstellar medium of the host quasar (An et al. 2010). The total projected size seen in this image is 2.6 kpc from the nucleus, although an extended envelope extends to about 5 kpc from the nucleus, the southernmost component seen in this image (An et al. 2010). Lower left: The CSS galaxy NGC6521 (J1755+6236) at a redshift of 0.0275 shows diffuse outer lobes with no prominent hot spots, indicating that the energy supply may have stopped (Polatidis 2009). The total projected size of the source defined by the outer lobes is 29 pc. Lower right: J2355+4950 associated with a galaxy at a redshift of 0.2379 shows hot spots along with diffuse emission on opposite sides and a well-defined radio jet (Polatidis et al. 1999; Taylor et al. 2000; Polatidis and Conway 2003; Polatidis 2009). The total projected size of the source defined by the outer lobes is 240 pc

It has now been shown that many of these objects are young - i.e. a significant verified prediction of Mutel and Phillips

Table 3 Proper motions of CSS and PS sources with measurements for hotspots

Source	Alt.	z	Sepn. pc (mas)	v_{sep}. c (mas/year)	Age year	Reference	Notes
J0000+4054	4C40.52		(40)	(<0.144)	>280	6	hs-hs
J0003+2129		0.45	21	0.15	500	18	hs-hs
J0003+4807			(4.8)	(<0.014)	>340	6	c-hs
J0005+0524		1.887	15	0.7	140	18	hs-hs
J0038+2303	B2 0035+22	0.0960	31	0.17	567	12,9	hs-hs
J0111+3906	S4 0108+388	0.6685	32	0.26	417	12,1,3,4	hs-hs
			41	0.04	1080	13	hs-hs
J0119+3210	4C 31.04	0.0602	60	0.33	550	5	c-hs
J0132+5620			(12.2)	(−0.005)	>4700	15	hs-hs;nr
			(11.5)	(0.028)	410	15	j-hs
			(10.5)	(0.060)	180	15	j-hs
			(2.4)	(−0.073)		15	j-hs
J0204+0903			(18)	(0.070)	240	6	c-hs
J0405+3803	B3 0402+379	0.0550	23	0.14	502	21	c1-hs
			7.3	0.0054		22	c1-c2
J0427+4133			(1.3)	(0.060)	20	6	c-hs?
J0518+4730			(3.1)	(−0.026)	~1200	15	c-hs;nr
			(1.9)	(0.030)		15	c-hs;nr
J0620+2102			(27)	(<0.013)	>2060	6	hs-hs
J0650+6001		0.455	40	0.39	360	20	hs-hs
			17	−0.37		20	c-hs
J0713+4349	B3 0710+439	0.5180	152	0.43	932	12,2,3,4	hs-hs
J0754+5324			(20)	(<0.009)	>2220	6	hs-hs
			(~8)	(0.060)		6	j-hs
J0831+4608	CORALZ	0.1311	10	0.14	245	25	hs-hs
J1035+5628	TXS 1031+567	0.4597	198	0.27	1836	12,3	hs-hs;nr
			190	0.86		12,3	hs-j?
J1111+1955	PKS 1108+201	0.2991	71	<0.14	>1620	6	hs-hs
			78	<0.19	>1360	6	hs-hs
J1143+1834			(6.9)	(<0.010)	>690	6	hs-hs
J1247+6723	B 1245+676	0.1073	15	0.23	190	12,9,23	hs-hs
J1317+4115	CORALZ	0.0662	4.2	<0.11	>130	25	hs-hs
J1324+4048		0.496	33	0.12	870	15	hs-hs
			28	2.2		15	hs-j
J1335+5844	4C 58.26		(0.57)				
			85	0.16	1800	15	hs-

Table 3 continued

Source	Alt.	z	Sepn. pc (mas)	v_{sep}. c (mas/year)	Age year	Reference	Notes
							hs-hs;nr
			75	2.86	90	15	j-hs;nr
J1407+2827	OQ 208	0.0766	11	0.108		16,12	hs-hs;nr
			9.5	0.134	255	16,12	hs-hs;nr
			1.8	−0.168		16	hs-j
J1414+4554	B3 1412+461	0.186	89	<0.14	>2030	6	hs-hs
J1415+1320	PKS1413+135	0.2467	31	0.80	130	6	c-j/hs
			7.6	1.10	22	6	c-j
J1511+0518		0.084	3.4	0.04	300	15,18	c-hs
			4.0			15,18	c-hs;nr
			5.3	0.15		15,18	c-hs;nr
J1546+0026		0.55	~35	−1.1		6	c-hs
J1609+2641	CTD 93	0.473	300	0.34	2200	7	hs-hs
J1723−6500	NGC 6328	0.0144	3	~0.1	91	24,12,9	hs-hs
J1734+0926	PKS 1732+094	0.735	96	<0.18	>1780	6	hs-hs
			101	0.25	1300	15	hs-hs;nr
J1755+6236	NGC6521	0.0274	20	<0.04		19	hs-hs
J1816+3457	B2 1814+34	0.245	~140			6	hs-hs;nr
J1826+1831			(14)	(0.037)	380	6	c-j
			(42)	(0.013)	3000	6	c-hs
J1845+3541	B 1843+356	0.7640	32	0.57	180	12,9	hs-hs
J1939−6342	PKS 1934-63	0.1813	130	0.26	1600	8,12	hs-hs
J1944+5448	B 1943+546	0.2630	153	0.37	1306	12,13,4,9	hs-hs
			166	0.27	1800	13	hs-hs
J1945+7055	TXS 1946+708	0.1008	56	<0.14		12	hs-hs
				<0.57	>200	11	hs-c
				0.29		12,11	j
				0.7-1.3		12,11	j
J2022+6136	B 2021+614	0.2270	25	0.2	440	10,9	hs-hs
J2203+1007		1.005	82	0.53	500	15,6	hs-hs;nr
			76	1.13	220	15	hs-j
J2355+4950	TXS 2352+495	0.2379	190	0.17	300	12,3,4	hs-hs
				0.4-1		3,12	hs-j

1. Owsianik et al. (1998); 2. Owsianik and Conway (1998); 3. Taylor et al. (2000); 4. Polatidis et al.

Why "Compact Symmetric Objects"?

A. C. S. READHEAD ET AL.

central component, and that the other two components are enhanced features in two oppositely directed jets of emitted material. This indicates that the basic ejection mechanism is two sided in at least some sources; it was pointed out in an earlier contribution that a similar structure is found in 3C390.3.
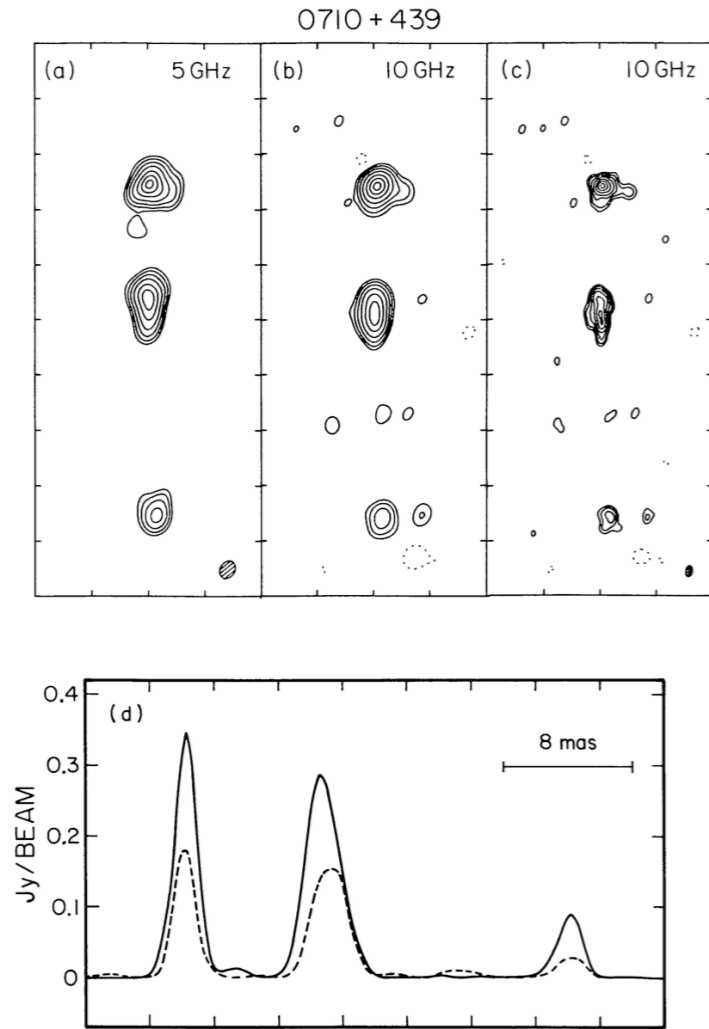

Fig. 2. Maps of 0710+439 (a) at 5 GHz, 1982 December; (b) at 10 GHz 1982 February, displayed with the same resolution as (a); (c) at 10 GHz, with full resolution; each box is 16 x 40 mas. (d) Profiles along the north-south axis of the maps in (a) and (b); solid line: 5 GHz, dashed line: 10 GHz.

THE COMPACT TRIPLES 0710+439 AND 2352+495: A NEW MORPHOLOGY OF RADIO GALAXY NUCLEI

J. E. CONWAY,[1] T. J. PEARSON, A. C. S. READHEAD, S. C. UNWIN, AND W. XU
Owens Valley Radio Observatory, Mail Code 105-24, California Institute of Technology, Pasadena, CA 91125

AND

R. L. MUTEL
Department of Physics and Astronomy, University of Iowa, Iowa City, IA 52242
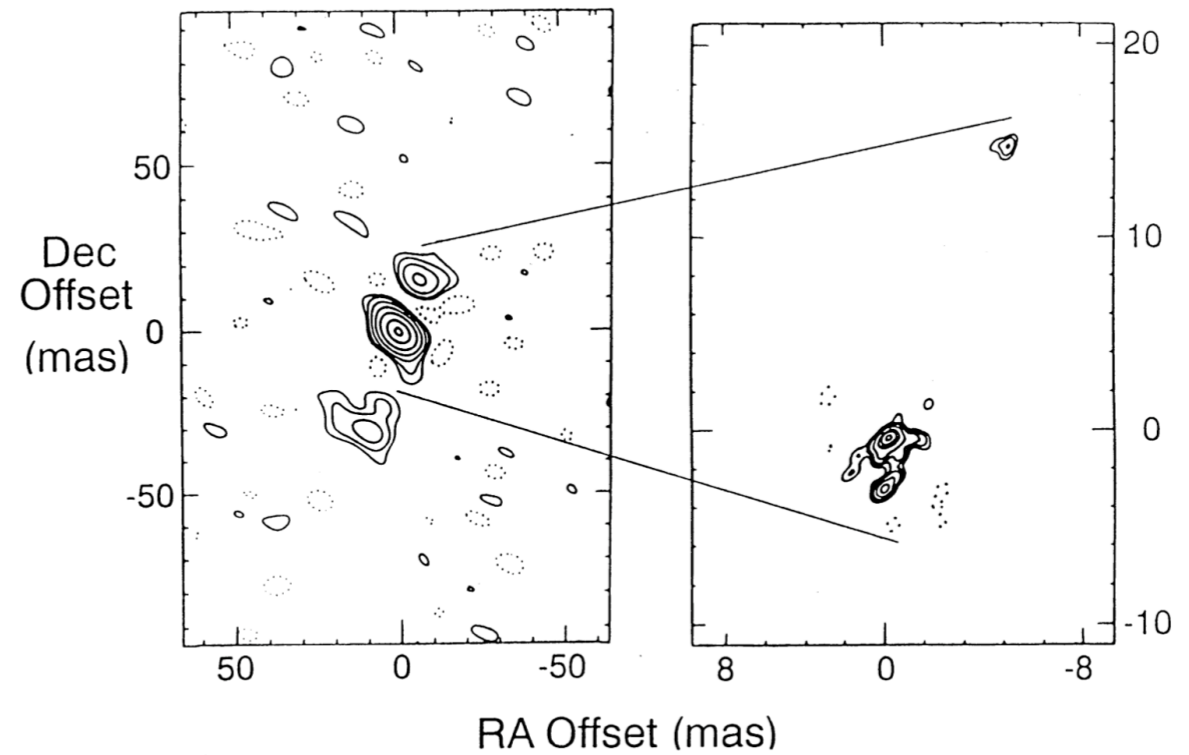Received 1991 December 10; accepted 1992 March 9

FIG. 9.—Maps of 2352+495 at 5 and 10.7 GHz. (a) Tapered 5 GHz map using only the inner 20 Mλ of UV data. Restoring beam is 9.66 by 6.40 mas position angle 47°.9, peak is 1.026 Jy beam^{-1}, contour levels are −2%, 2%, 4%, 8%, 16%, 32%, 64%, and 95% of peak. (b) Full-resolution 10.7 GHz map, showing components A and B only, C is detected but is to the south of this field. Restoring beam is 0.7 by 0.5 mas position angle −40°. Peak flux density is 141.2 mJy beam^{-1}. Contour levels are −3%, 3%, 6%, 10%, 20%, 40%, 60%, and 90% of the peak.

Evidence for a Population of Short-Lived Powerful Radio Galaxies

A.C.S. Readhead, W. Xu, T.J. Pearson (Caltech), P.N. Wilkinson, A. Polatidi (NRAL, Jodrell Bank)

It has recently become clear that the unusual "compact triple" radio galaxy 0710+439, discovered almost a decade ago (Readhead, Pearson & Unwin 1984 IAU Symp. 110, 131), is the prototype member of a distinct class of activ galaxies (Conway *et al.* 1992, ApJ, 396, 62) that we call "Compact Symmetric or CS objects. The distinguishing features of this class are: (1) the radio structur is symmetrically distributed about the center of activity; (2) the overall exten of the radio structure is typically a few hundred parsecs; (3) the radio emissio is not strongly beamed; (4) the high-frequency radio spectra are steep; (5) th objects have low polarization; and (6) the objects display weak variability. The symmetry observed in these objects contrasts strongly with the asymmetric nuclear structure observed in most radio-loud objects, be they core-dominated flat-spectrum quasars, lobe-dominated steep-spectrum quasars, lobe-dominated steep-spectrum galaxies, or the majority of steep-spectrum compact objects.

Possible explanations for CS objects include: (1) they are precursors of FR-II objects, (2) they are "frustrated jets," or (3) they are young objects (1000–10,000 yr).

We analyze multifrequency observations of the CS object 2352+495, identi-fied with a galaxy at a redshift of 0.518, and show that the radio activity in this object is almost certainly short-lived - i.e., this is a "young" radio object. We use this result, in combination with our observations of two complete samples, to demonstrate that the most plausible explanation is that the CS objects are a previously unsuspected class of short-lived, powerful radio galaxies.

TWO-SIDED EJECTION IN POWERFUL RADIO SOURCES: THE COMPACT SYMMETRIC OBJECTS

P. N. WILKINSON AND A. G. POLATIDIS
University of Manchester, Nuffield Radio Astronomy Laboratories, Jodrell Bank, Macclesfield, Cheshire SK11 9DL, UK

AND

A. C. S. READHEAD, W. XU, AND T. J. PEARSON
California Institute of Technology, Owens Valley Radio Observatory, 105-24, Pasadena, CA 91125

ABSTRACT

We present VLBI images of the compact high-luminosity radio galaxy 2352+495 that show symmetric structure on either side of a prominent central core. This contrasts strongly with the asymmetric nuclear struc-ture exhibited by the great majority of powerful extragalactic sources. The outer structure of 2352+495 takes the form of two "mini-lobes" containing hot spots; in this respect this compact radio galaxy resembles extended radio galaxies, but its overall size, ~150 pc, is ~1000 times smaller. A reanalysis of existing data on the radio galaxy 0710+439 shows similar compact structure, and together these VLBI images confirm the existence of a class of two-sided compact symmetric objects (CSOs). We show that, in contrast to nuclear radio sources in other powerful objects, the observed structure of CSOs is not dominated by relativistic beaming effects. It is likely that many objects previously classified as "compact doubles" will prove to be CSOs when mapped with VLBI with high dynamic range.

Subject headings: galaxies: active — galaxies: individual (0710+439, 2352+495) — galaxies: nuclei — radio continuum: galaxies

Although our systematic morphological study of CSOs is still in its early stages, we can identify broad defining charac-teristics, namely, (1) two or more components, separated by 10–1000 pc, either straddling a central core or with other com-pelling morphological evidence for symmetry such as outer hot spots, and (2) no emission on scales greater than 1000 pc or only very faint emission. The morphologies of 0710+439 and 2352+495, the population statistics of CSOs and CDs in the PR and CJ1 surveys, and the component proper-motion limits for the core and hot spots derived by Conway et al. (1992) confirm that relativistic beaming does not play a major role in determining the radio properties of CSOs. It is likely that many compact double sources will prove to be CSOs when higher dynamic range VLBI maps are made.

SPITZER MID-INFRARED SPECTROSCOPY OF COMPACT SYMMETRIC OBJECTS: WHAT POWERS RADIO-LOUD ACTIVE GALACTIC NUCLEI?

KYLE W. WILLETT[1], JOHN T. STOCKE[1], JEREMY DARLING[1], AND ERIC S. PERLMAN[2]
[1] Center for Astrophysics and Space Astronomy, Department of Astrophysical and Planetary Sciences, UCB 391, University of Colorado, Boulder, CO 80309-0391, USA
[2] Florida Institute of Technology, Physics and Space Sciences Department, 150 West University Boulevard, Melbourne, FL 32901, USA

ABSTRACT

We present low- and high-resolution mid-infrared (mid-IR) spectra and photometry for eight compact symmetric objects (CSOs) taken with the Infrared Spectrograph on the *Spitzer Space Telescope*. The hosts of these young, powerful radio galaxies show significant diversity in their mid-IR spectra. This includes multiple atomic fine-structure lines, H_2 gas, polycyclic aromatic hydrocarbon (PAH) emission, warm dust from $T = 50$ to 150 K, and silicate features in both emission and absorption. There is no evidence in the mid-IR of a single template for CSO hosts, but 5/8 galaxies show similar moderate levels of star formation ($<10\,M_\odot$ yr^{-1} from PAH emission) and silicate dust in a clumpy torus. The total amount of extinction ranges from $A_V \sim 10$ to 30, and the high-ionization [Ne v] 14.3 and 24.3 μm transitions are not detected for any galaxy in the sample. Almost all CSOs show contributions both from star formation and active galactic nuclei (AGNs), suggesting that they occupy a continuum between pure starbursts and AGNs. This is consistent with the hypothesis that radio galaxies are created following a galactic merger; the timing of the radio activity onset means that contributions to the IR luminosity from both merger-induced star formation and the central AGN are likely. Bondi accretion is capable of powering the radio jets for almost all CSOs in the sample; the lack of [Ne v] emission suggests an advection-dominated accretion flow mode as a possible candidate. Merging black holes (BHs) with $M_{\rm BH} > 10^8\,M_\odot$ likely exist in all of the CSOs in the sample; however, there is no direct evidence from these data that BH spin energy is being tapped as an alternative mode for powering the radio jets.

Key words: accretion, accretion disks – galaxies: evolution – galaxies: jets – infrared: galaxies – radio continuum: galaxies
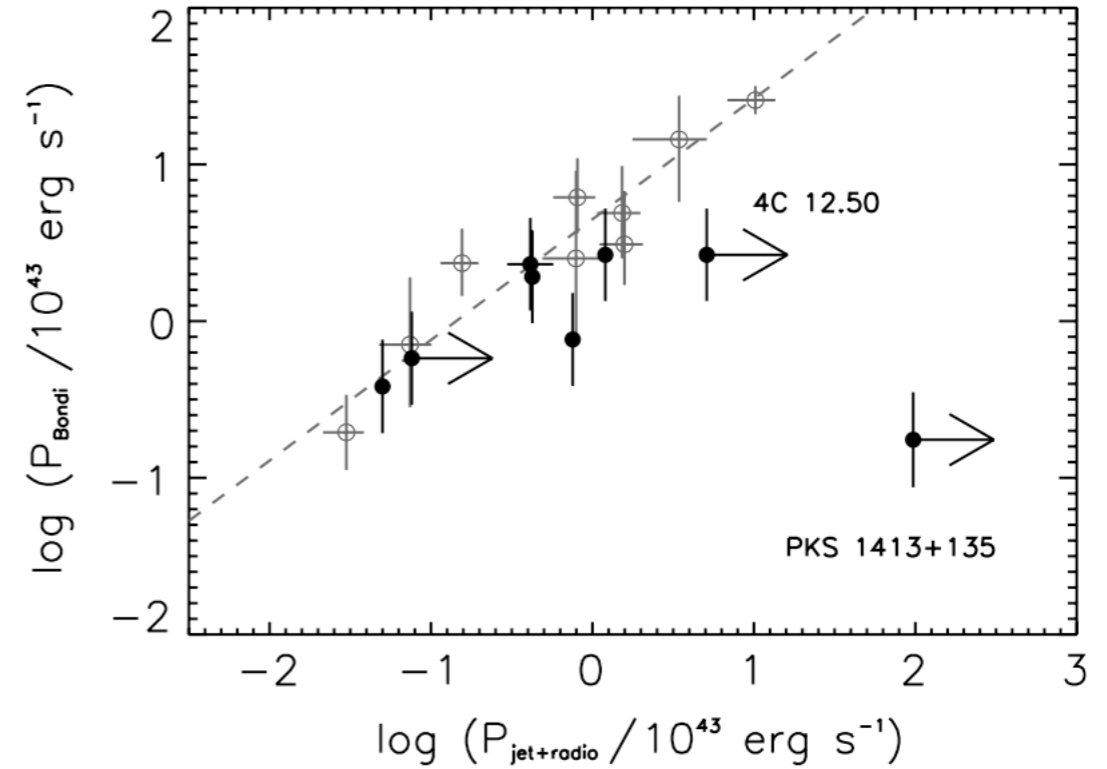
Figure 14. Bondi accretion power as a function of the combined jet mechanical power and radio luminosity. The black filled dots are CSOs, while the gray dots are X-ray luminous elliptical galaxies from Allen et al. (2006). Arrows show the limits on CSOs without constrained $t_{\rm age}$. The dashed line is a linear fit to the X-ray ellipticals; we label CSOs that deviate significantly from this fit.

4. Category 4 objects have *no* discernible emission features, with the only break in a continuum that can be fit with a single power law the silicate absorption at 9.7 and 18 μm. PKS 1413+135 is the only CSO in the sample with these basic blazar characteristics.

MULTIFREQUENCY VLBI OBSERVATIONS OF PKS 1413+135:
A VERY YOUNG RADIO GALAXY

ERIC S. PERLMAN

USRA/LHEA, Mail Code 660.2, Goddard Space Flight Center, Greenbelt, Maryland 20771
Electronic mail: perlman@rosserv.gsfc.nasa.gov

CHRIS L. CARILLI

Smithsonian Astrophysical Observatory, 60 Garden Street, Cambridge, Massachusetts 02138

JOHN T. STOCKE

Center for Astrophysics and Space Astronomy, University of Colorado, Campus Box 389, Boulder, Colorado 80309

JOHN CONWAY

Onsala Space Observatory, S-43992 Onsala, Sweden
Received 1995 December 27; revised 1996 January 24
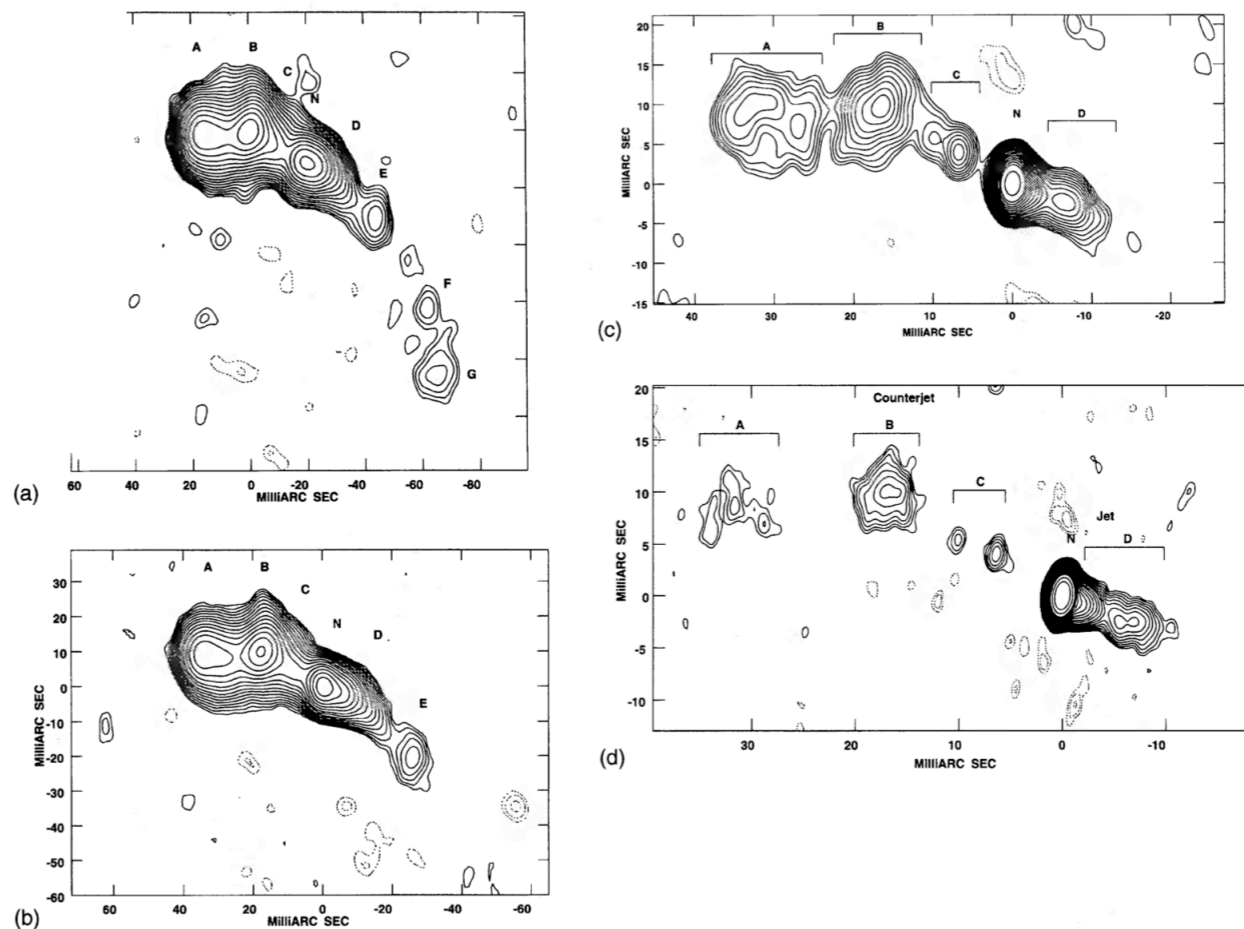
FIG. 1. Naturally weighted VLBA images of PKS 1413+135 at 18, 13, 6, and 3.6 cm. The map contours are at $(-2, -1.4, -1, 1, 1.4, 2, 2.8, 4, 5.7, 8, 11, 16, 22, 32, 45, 64, 91, 128, 182, 256, 512, 1024) \times C$. The panels and C values are: (a) 18 cm, $C = 6 \times 10^{-4}$ Jy/beam; (b) 13 cm, $C = 6 \times 10^{-4}$ Jy/beam; (c) 6 cm, $C = 6 \times 10^{-4}$ Jy/beam; and (d) 3.6 cm, $C = 4 \times 10^{-4}$ Jy/beam.
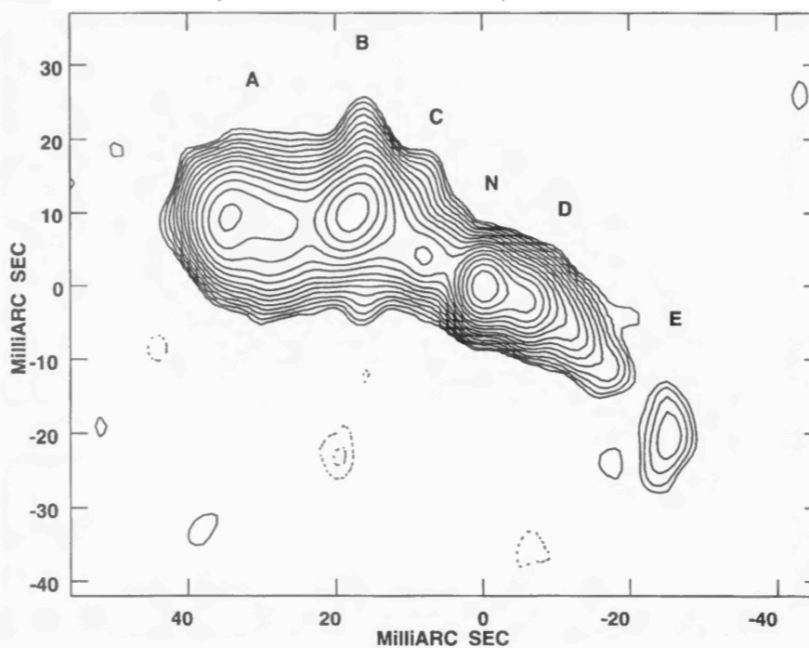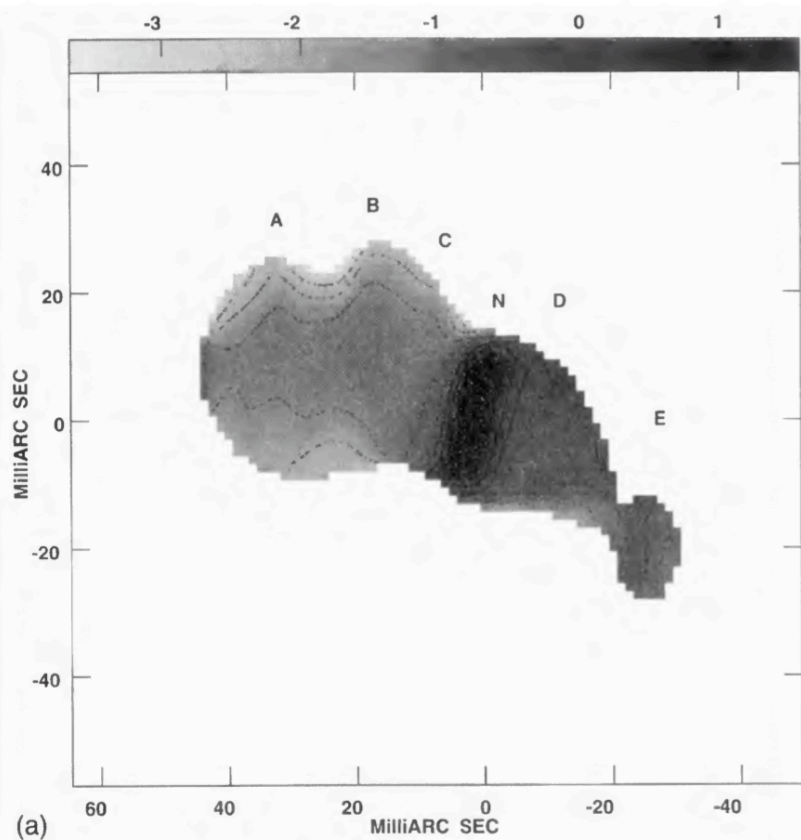
FIG. 3. Uniformly weighted VLBA image of PKS 1413+135 at 13 cm. This image shows some of the separation into individual components seen more clearly by the higher-resolution, short-wavelength data. Contours are at $(-2, -1.4, -1, 1, 1.4, 2, 2.8, 4, 5.7, 8, 11, 16, 22, 32, 45, 64, 91, 128, 182, 256, 512, 1024) \times 5 \times 10^{-4}$ Jy/beam.

Symmetric Achromatic Variability in Active Galaxies: A Powerful New Gravitational Lensing Probe?

H. K. Vedantham[1], A. C. S. Readhead[1], T. Hovatta[2,3,4], T. J. Pearson[1], R. D. Blandford[5], M. A. Gurwell[6], A. Lähteenmäki[2], W. Max-Moerbeck[7], V. Pavlidou[8], V. Ravi[1], R. A. Reeves[9], J. L. Richards[1], M. Tornikoski[2], and J. A. Zensus[7]
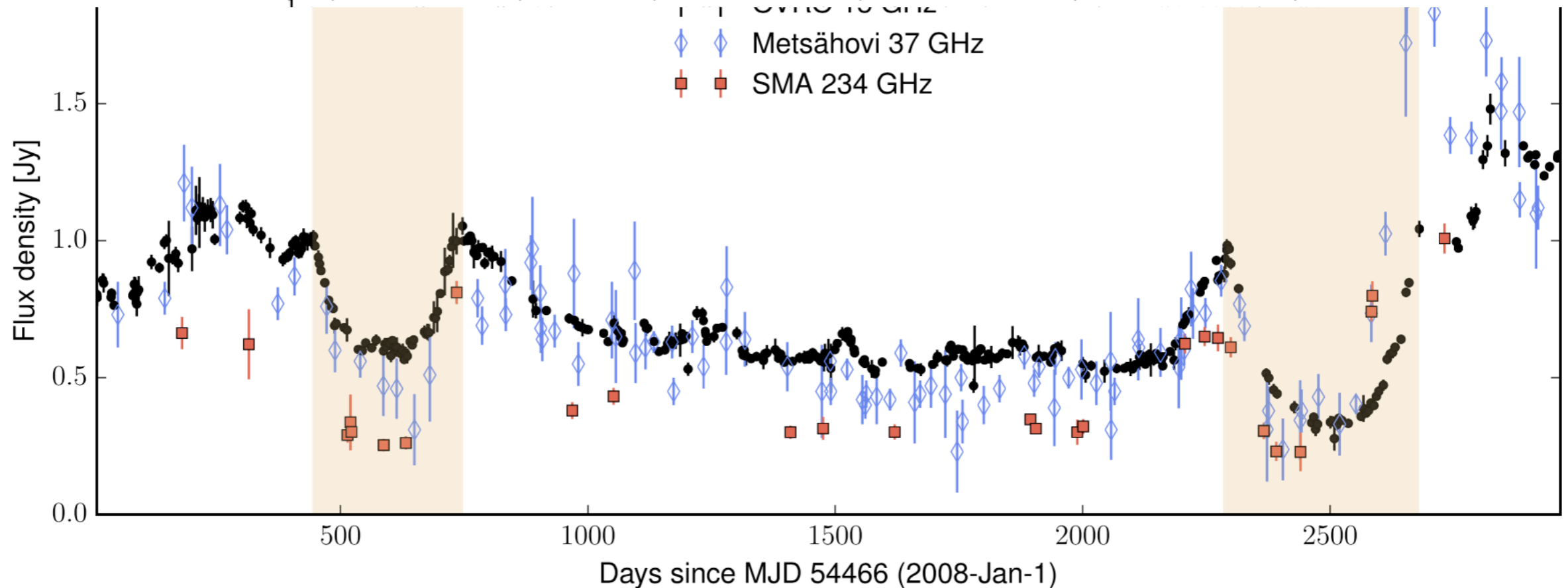
Figure 1. Multifrequency light curves of J1415+1320 showing symmetric achromatic variability (SAV). The roughly 1-year-long U-shaped SAV events in 2009 a...
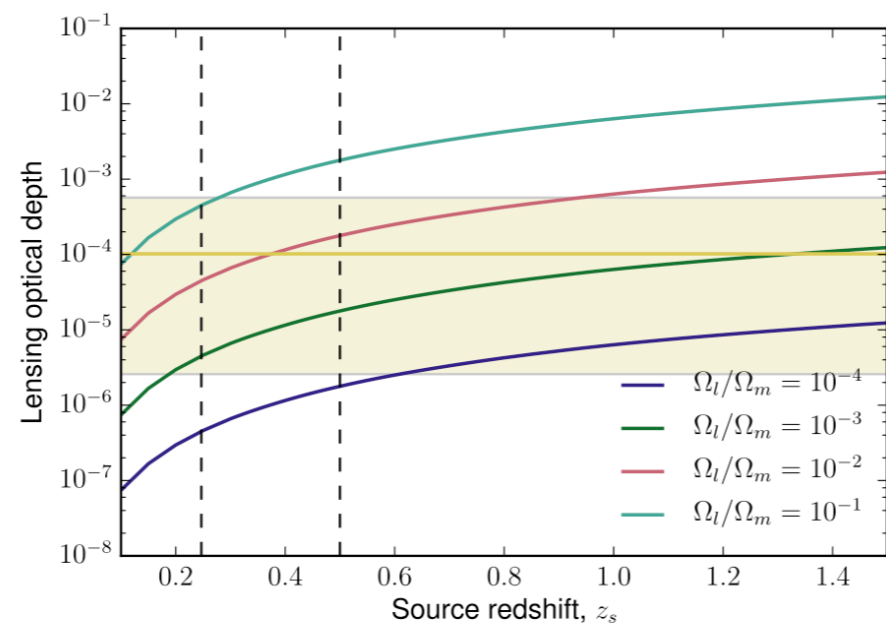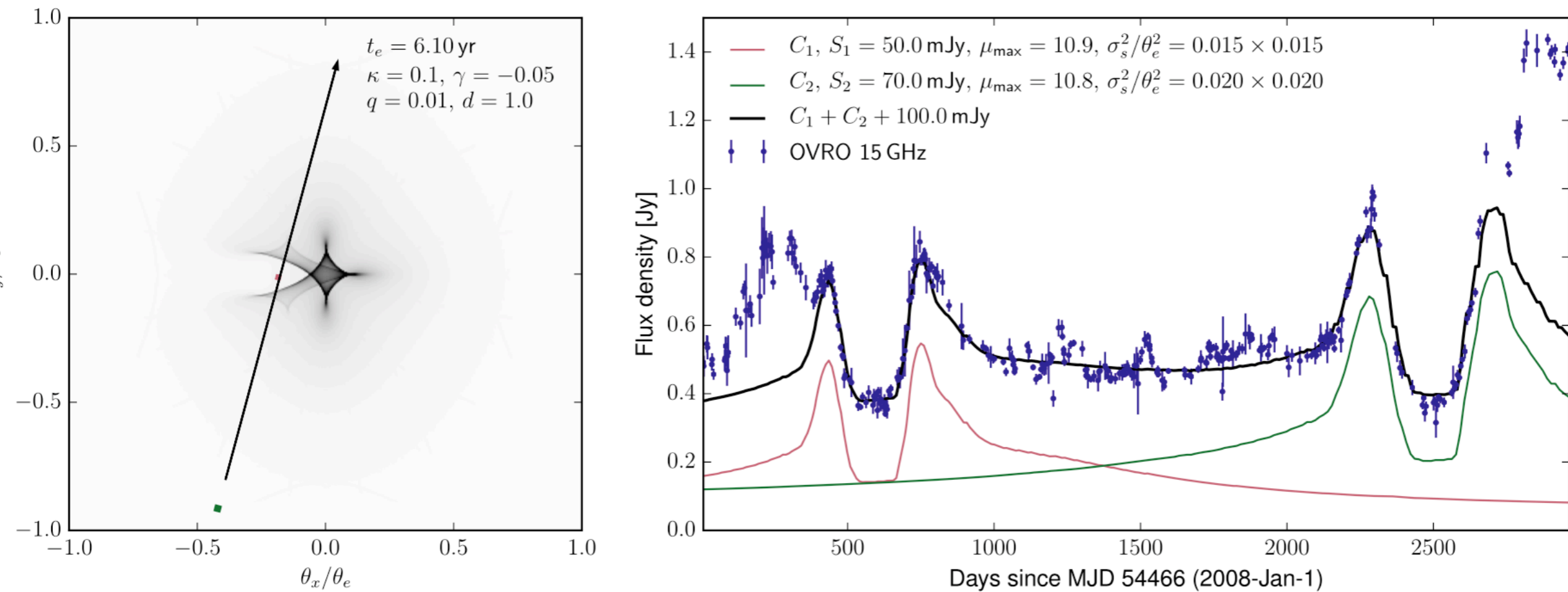
Figure 7. Fraction of lines of sight intercepted by the putative lens population (lensing optical depth) as a function of source redshift. The curves correspond to cases where different fractions of the cosmological matter density are in the lenses. The horizontal yellow line corresponds to the observed probability of intercepting a lens (based on just one sample, J1415+1320), and the shaded region is the corresponding 95% confidence interval assuming Poisson statistics.

https://doi.org/10.3847/1538-4357/aa774

CrossMark

The Peculiar Light Curve of J1415+1320: A Case Study in Extreme Scattering Events

H. K. Vedantham[1], A. C. S. Readhead[1], T. Hovatta[2,3,4], L. V. E. Koopmans[5], T. J. Pearson[1], R. D. Blandford[6], M. A. Gurwell[7], A. Lähteenmäki[2,3], W. Max-Moerbeck[8], V. Pavlidou[9], V. Ravi[1], R. A. Reeves[10], J. L. Richards[1], M. Tornikoski[2], and J. A. Zensus
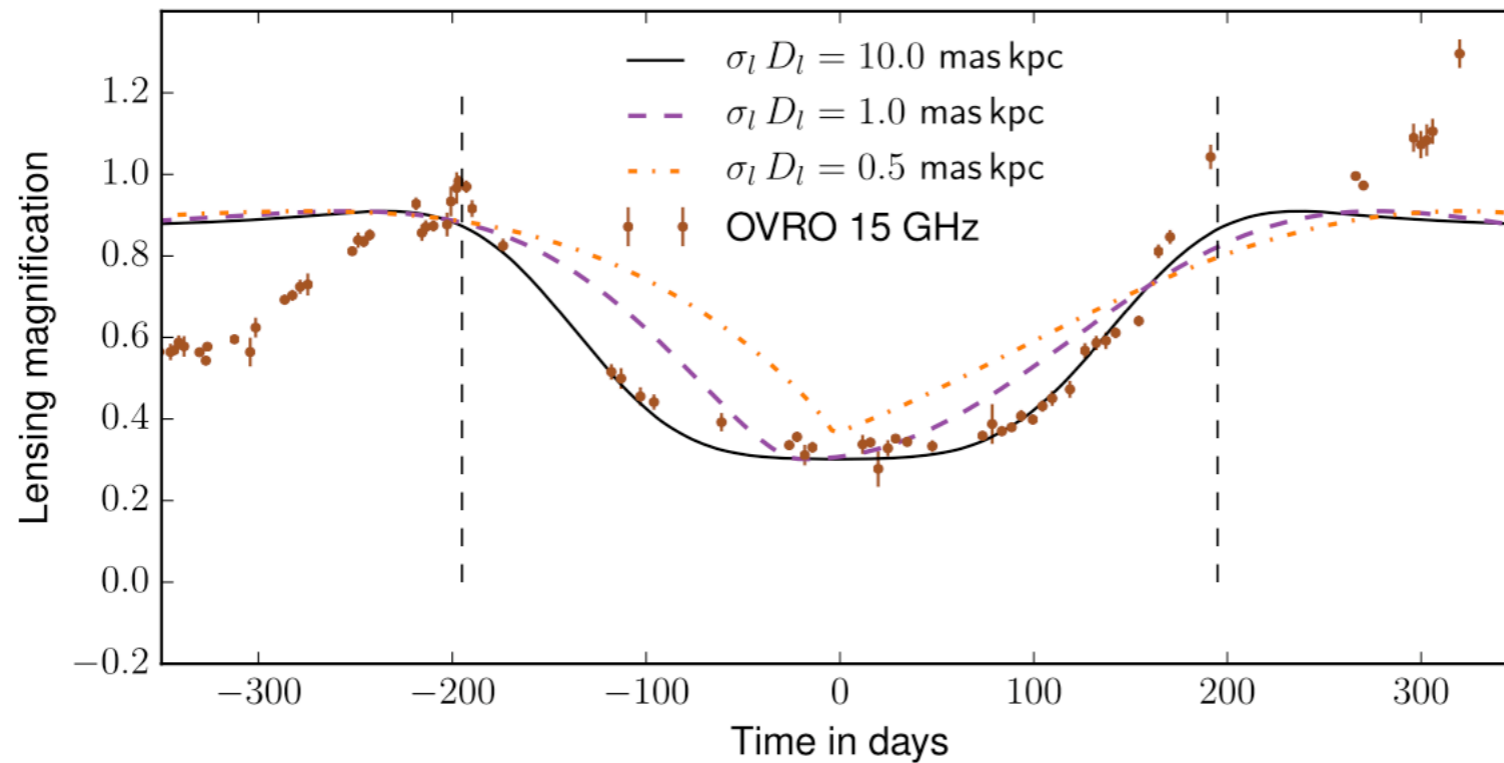
The Relativistic Jet Orientation and Host Galaxy of the Peculiar Blazar PKS 1413+135

A. C. S. Readhead[1], V. Ravi[1], I. Liodakis[2], M. L. Lister[3], V. Singh[4], M. F. Aller[5], R. D. Blandford[2],
I. W. A. Browne[6], V. Gorjian[7], K. J. B. Grainge[6], M. A. Gurwell[8], M. W. Hodges[1], T. Hovatta[9,10], S. Kiehlmann[11],
A. Lähteenmäki[10,12], T. Mcaloone[6], W. Max-Moerbeck[13], V. Pavlidou[11], T. J. Pearson[1], A. L. Peirson[2],
E. S. Perlman[14], R. A. Reeves[15], B. T. Soifer[16], G. B. Taylor[17], M. Tornikoski[10], H. K. Vedantham[18], M. Werner[7],
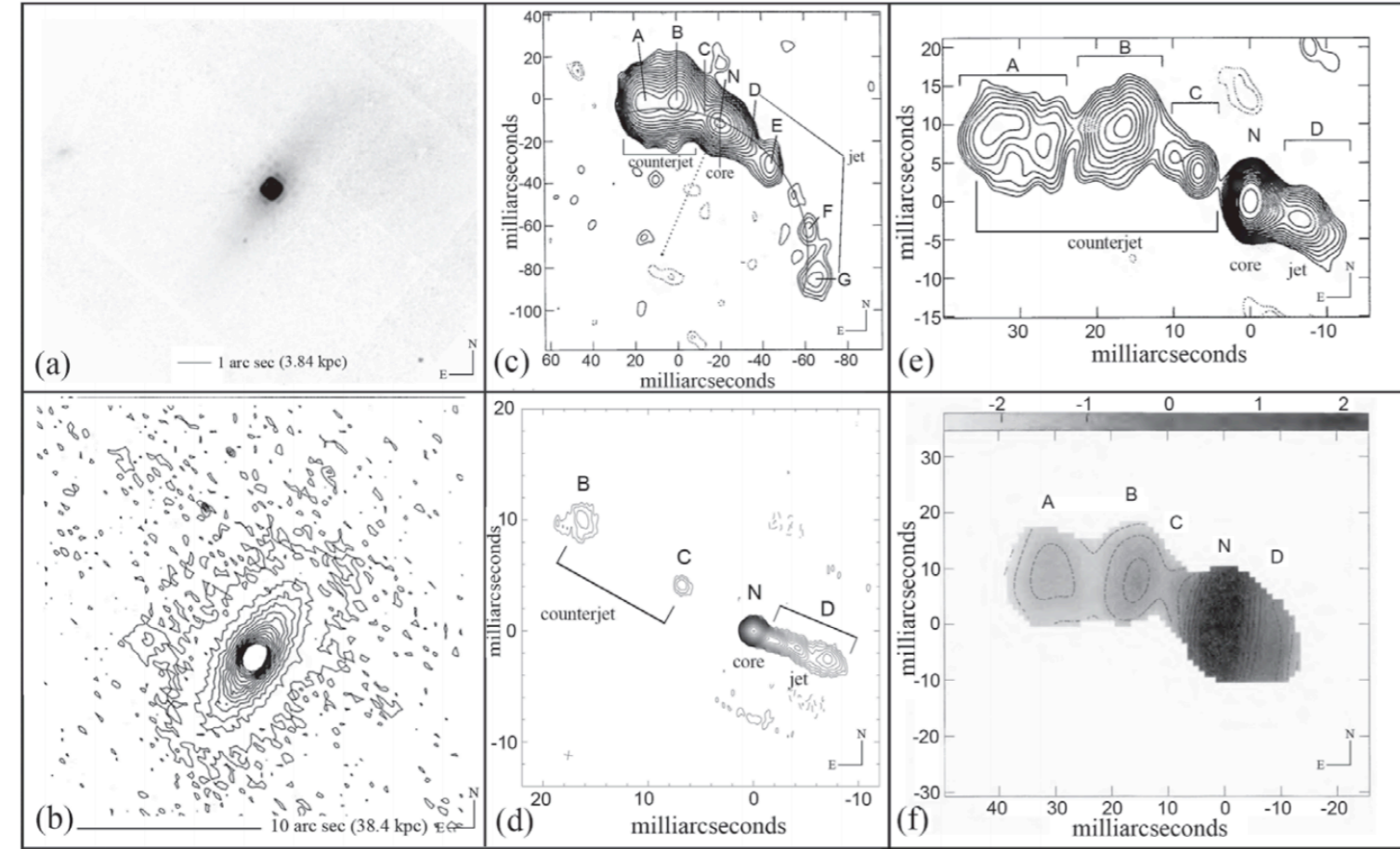P. N. Wilkinson[6], and J. A. Zensus[19]

Figure 4. Six images of the PKS 1413+135 and spiral galaxy system that show the near-orthogonality projected on the sky of the optical/IR spiral disk plane and the nuclear radio jet and counterjet. (a) Mosaicked HST NICMOS image of Perlman et al. (2002). (b) *R*-band William Herschel Telescope image from McHardy et al. (1991). (c) 1.67 GHz VLBI image from Perlman et al. (1996) showing the total extent of the radio structure that has been observed. The contours are spaced by a factor of $\sqrt{2}$ in brightness. No features on scales greater than ~110 mas have been observed. Component N marks the nucleus or radio core. The bright counterjet is designated by A, B, and C. This image shows the curving structure of the radio emission. The inscribed arc is centered on a point ~70 mas southeast of the radio core N to illustrate the Einstein radius of a ~$10^9\,M_\odot$ gravitational lens (see Section 4.2). (d) VLBI map made from stacking 15 GHz MOJAVE images from 23 epochs between 1995 July 16 and 2011 May 26, showing the bright core and the emerging jet D and inner counterjet component C. The contours are spaced by a factor of $\sqrt{2}$ in brightness with the lowest positive contour at 0.243 mJy/beam (image from Pushkarev et al. 2017 but with different contour levels). (e) 5 GHz image from Perlman et al. (1996) showing a clear bend in the counterjet at component B. The contours are spaced by a factor of $\sqrt{2}$ in brightness. (f) 2.3 GHz to 5 GHz spectral index map from Perlman et al. (1996). The letters designating components in panels (c)–(f) all refer to the same components.
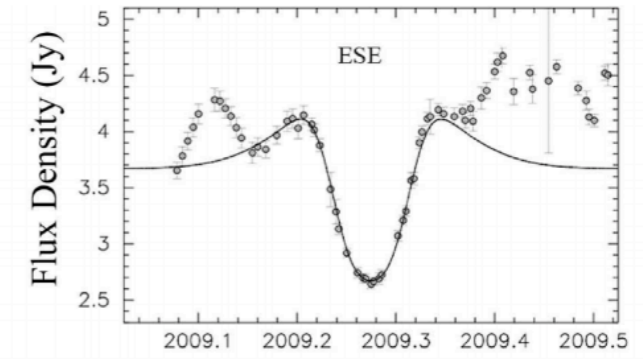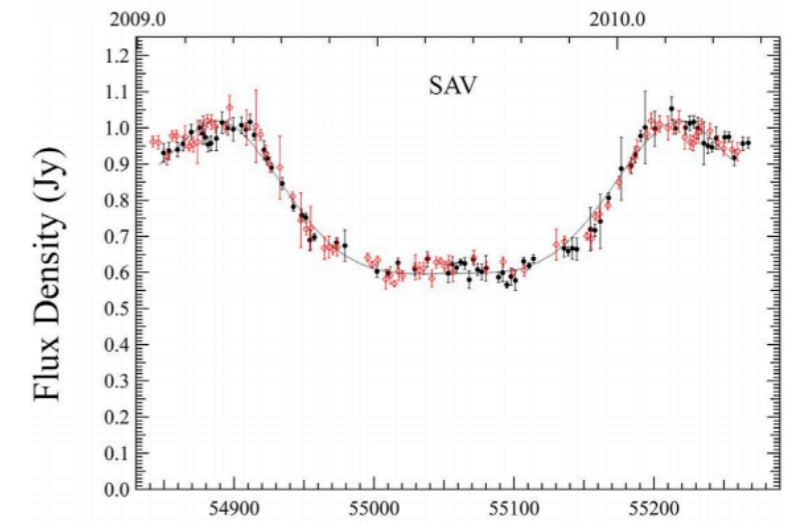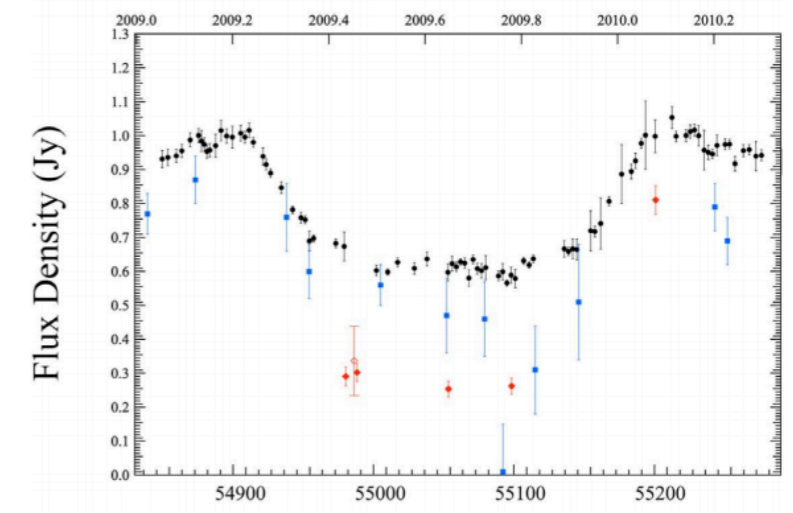
Figure 8. Symmetry in ESE and SAV. (a) Example of ESE symmetry in the blazar 2023+335 (Pushkarev et al. 2013) from the 40 m Telescope with the black curve showing the fit of the ESE model. (b) The first SAV identified (in PKS 1413+135) on the 40 m Telescope monitoring Paper 1: black dots—original data; red diamonds—original data in reverse time order, demonstrating the high degree of symmetry. Gray curve from Paper 1. Similarities between ESE and SAV are clear. However, ESE has been definitively ruled out as the origin of SAV (see text). (c) from 15 to 230 GHz: the black dots are from the Owens Valley Radio Observatory at 15 GHz, the blue squares are from the Metsähovi Radio Observatory, the red filled triangles are from the Submillimeter Array (SMA) at 230 GHz, and the red open triangle is from the SMA at 345 GHz.

The original classification criteria for CSOs were three: (i) overall projected diameter smaller than ~ 1 kpc, (ii) an identified center of activity, and (iii) symmetric jet structure about the center. However there has been much confusion in the literature and erosion of the value of the CSO classification due to misclassified CSOs, because many jets contain compact bright features outside of the core, resulting in a GPS total spectrum and a 'compact double' appearance, and some relativistically boosted objects with jet axes aligned close to the line of sight appear symmetric because the approaching jet is projected on both sides of the core. We propose adding two new criteria to the CSO classification criteria based on (iv) the radio variability and (v) the apparent velocities of bright features moving along the jets. We are engaged in compiling a comprehensive catalog of CSOs drawn from the literature based on these five criteria.

Comprehensive literature search:

1. Papers that mention CSO's in the title or abstract, then follow-up of other papers mentioned
2. GPS sources that have VLBI images
3. Assembled images, spectra, variability images

A Comprehensive Catalog of Compact Symmetric Objects

S. Kiehlmann,[1,2] M.L. Lister,[3] Sandra O'Neill,[4] T. J. Pearson,[4] A.C.S Readhead,[4] Evan Sheldahl,[5] Aneta Siemiginowska,[6] G.B. Taylor,[5] and P.N. Wilkinson[7]

Papers Reviewed (143)

CSO candidates considered (2077)

Bone Fide CSOs (77)

Candidate "A" sources (170)

Candidate "C" sources that need VLBI or better VLBI (914)

Rejected CSOs (916: 82 previously named CSOs)

UNIWERSYTET
MIKOŁAJA KOPERNIKA
W TORUNIU

Institute of Astronomy, Nicolaus Copernicus University, Toruń, Poland

Evidence of Recurring Activity in Active Galaxies Associated with Compact Symmetric Objects

S. O'Neill,[1] S. Kiehlmann [iD],[2,3] A.C.S. Readhead,[1] M.L. Lister,[4] T. J. Pearson,[1] E. Sheldahl,[5] A. Siemiginowska,[6] G.B. Taylor,[5] and P.N. Wilkinson[7]

Papers Reviewed (63)

Recurrent activity candidates considered (206)

Bone Fide CSOs (9)

Bone Fide MSOs (6)

Thank You!

UNIWERSYTET
MIKOŁAJA KOPERNIKA
W TORUNIU

Institute of Astronomy, Nicolaus Copernicus University, Toruń, Poland